International Journal of Heat and Mass Transfer 110 (2017) 778–782

Contents lists available at ScienceDirect

International Journal of Heat and Mass Transfer

journal homepage: www.elsevier.com/locate/ijhmt

Water evaporation in parallel plates

Shu Soma, Tomoaki Kunugi *

Department of Nuclear Engineering, Kyoto University, Kyoto-Daigaku Katsura, Nishikyo-ku, Kyoto 615-8540, Japan

ARTICLE INFO

Article history:
Received 14 November 2016
Received in revised form 24 February 2017
Accepted 23 March 2017
Available online 30 March 2017

Keywords:
Evaporation
Meniscus
Curvature
Contact line

ABSTRACT

The influence of macroscopic curvature on evaporation of the meniscus between parallel glass plates standing on purified water pool has been quantified experimentally. The gap distance between the plates was short compared to the capillary length, so the surface curvature increased with decrease of the gap distance. The meniscus was not heated and the thermal relaxation time of the plates estimated to be small. The evaporation rate and flux, obtained from time-evolution of vapor pressure in an experimental enclosure, could increase with increase of the curvature between the plates. Based on the comparison among the existing data including ours, it was clear the evaporation rate and flux could be organized by a curvature, not a perimeter (a contact-line length).

1. Introduction

The thermal-hydraulic characteristics accompanying the phase change phenomena in a micro-channel are of interest due to the higher heat-transfer augmentation and applicability to the micro-scale cooling devices. If we can assume that liquid wets solid wall perfectly, liquid film near a contact line can be divided into three regions characterized by two different forces: a disjoining pressure and a capillary force. The macroscopic region of a meniscus, which is called an "intrinsic meniscus" [1] or "macro region" [2], is defined by both an apparent contact angle and a macroscopic curvature, and the capillary force due to the macroscopic curvature is dominant in there. The perfectly wetted solid wall is covered by a very thin liquid layer at thermodynamically equilibrium, so-called an "equilibrium thin film", where water could not evaporate due to the dispersion force between the liquid molecules and the atoms of wall material. The interface pressure which deviates from the saturation one due to the intermolecular force is called the disjoining pressure. The disjoining pressure is inversely proportional to the cube of the film thickness in the case of planer film [3,4]. A transition region between the macro region and the equilibrium thin film is called a "micro region" [2,5]. The effect of disjoining pressure is weak and the thermal resistance to heat conduction is so small [6], so the evaporation is high at this region. These divided regions are often applied to the scene of the nucleate boiling. In this case, as well as the evaporation of the meniscus, the contact line may play an important role for the heat transport from the heating wall to the vapor-liquid interface, called a "microlayer" [7]. In addition, the micro region also appears at the scene of the evaporation of liquid droplet which partially or completely wets the substrate [8]. Therefore, it is important to understand the hidden fundamental physics behind such phenomena for further improvements of the engineering design of the evaporator etc. as well as the theoretical and numerical models which predict heat and mass transfer in two-phase systems.

While the macroscopic curvature of the interface at the macro region is regarded as an inverse of the radius of the system (i.e., an inner radius of the channel, a distance of the gap, etc.), the curvature varies near the contact line due to the existence of the equilibrium thin film. The phase change phenomena is strongly dependent on the curvature of the interface from the point of view of the thermodynamics [9–11] and the heat and mass transport process near the contact line. It was reported that the pressure gradient due to the change of the meniscus shape could be sufficient to suck the liquid required for evaporation [1]. The liquid flow was driven by the capillary pressure gradient and the disjoining pressure gradient. In order to describe the heat flow from the superheated wall to the evaporating meniscus, two independent models were presented [12]: one was derived from the heat conduction equation, and the other was from the free boundary problem. The heat transfer coefficient in the liquid film could be derived from Hertz-Knudsen-Schrage equation [13], where the gradient of the disjoining pressure was assumed to be sufficient to suck the liquid. The models of the evaporating meniscus using the modified Young-Laplace equation have been proposed by many researchers [14–20], on the other hand the dynamics of the triple contact line has not been clear in those models because they assumed a static

* Corresponding author.
E-mail address: kunugi@nucleng.kyoto-u.ac.jp (T. Kunugi).

http://dx.doi.org/10.1016/j.ijheatmasstransfer.2017.03.085
0017-9310/

meniscus. It was pointed out in [15] that those models were deficient in the three-phase interaction at the contact line. The experimental studies on the evaporation of the liquid in the mouse of the funnel [21–23] and capillary tubes [24–28] were reviewed in [29]. It was discussed that the thermocapillary convection could occur underneath the interface driven by the evaporation. The evaporation rate and flux from the meniscus of the volatile liquid in the capillary tubes of various diameters were obtained [24], and also the temperature distributions at the outer surface of the capillary tubes were measured by an IR camera [25]. It was found that the evaporation rate linearly decreased and the flux increased as the diameter decreased. They argued that this trend confirmed that the evaporation from the micro region was large, and suggested that the linearity of the evaporation rate with the tube diameter was due to the variation of the contact-line length. Based on the IR measurements, they also showed that the smaller tube diameter led the stronger evaporation.

In this paper, the influence of the macroscopic curvature on the evaporation rate of water from the meniscus was investigated. In the previous experiments conducted by using capillary tubes [24], they could not evaluate individually the effect of the curvature and that of the contact-line length on the evaporation. This is because they changed the tube diameter, i.e., the contact-line length and the macroscopic curvature were simultaneously changed. The evaporation rate and flux could be affected by the macroscopic curvature of the meniscus, however, there is no experimental study on how much the curvature of the meniscus influences the evaporation rate in detail. Moreover, there are few experimental studies on the evaporation rate and flux from the meniscus in the vertically standing parallel plates, not the tubes, as far as we know. In addition, many studies have not investigated water, so the data acquisition of the water evaporation is not sufficient till today. In this study, therefore, two parallel glass plates were used to evaluate individually the effect of the curvature and that of the contact-line length, and the purified water was chosen as a working fluid. The influence of the macroscopic curvature on the evaporation rate of water at the meniscus was discussed.

2. Experimental apparatus and procedure

Evaporation rates, evaporation fluxes and contact angles of the meniscus between two glass plates have been experimentally obtained. The test section as shown in Fig. 1(a) consisted of two glass plates as the test plate and two Polystyrene transparent plates as the edge-plate standing on a cylindrical pool filled with a purified water. The size of the glass plate was the width of 26 mm, height of 76 mm and the thickness of 1.0 mm. In the experiment, the gap distance between the parallel glass plates was adjusted by a thickness gauge of 0.30–1.50 mm. In other words, the macroscopic curvature of the meniscus was controlled. While the macroscopic curvature could be set to the desired value, the variation of the perimeter of the gap was so small (only a few% of it) in this study, compared to the previous studies using the tubes as the test section. Therefore, the effect of the curvature and that of the contact-line length were evaluated individually.

Prior to the experiments, the oil molecules adsorbed on the glass plates were wiped out by using ethanol, rinsed by the purified water, and then dried. The thickness gauge was inserted into the gap between the glass plates to adjust the gap distance. This test section was installed and stabilized in the cylindrical pool which was cleaned by ethanol and rinsed by the purified water. The purified water was poured to the pool gently, and then water rose up to its equilibrium position in the gap between the glass plates due to the capillary force. The purified water poured into the pool was boiled in order to degas and then was cooled to the room temperature, which was kept at 295 ± 1 K. After pouring the purified water, the nonvolatile oil (rapeseed oil) was poured on the water pool to prevent the evaporation of the water surface. The oil was kept from coming into the meniscus. The test section has no internal/external heater. This test section was installed in an acrylic transparent enclosure covered with the thermal insulator, so the system was thermally isolated from the outside environment. The enclosure was connected to an auxiliary tank for the evacuation of air from the enclosure by a vacuum pump as shown in Fig. 1(b). After evacuating air from the tank and setting the desired pressure to it, the connecting valve was opened, and the pressure between the enclosure and the tank was equalized. After the equalization, the increase of the pressure in the enclosure caused by the evaporation from the meniscus was measured by a differential pressure gauge. The output of the differential pressure gauge (KEYENCE Corp.) was logged by the data logger (KEYENCE Corp.). The evaporation rate was evaluated by the time-evolution of the differential pressure. In order to quantify the evaporation rate, the evaporation process was assumed as a diffusion phenomenon, and a kind of solution of the diffusion equation was used as a correlation function:

$$f(t) = a \times \mathrm{erfc}(b/\sqrt{t}). \quad (1)$$

Here, a (Pa) and b (min$^{1/2}$) are fitting parameters. t (min) is time period after the reference time. In this study, the pressure time-evolution data at 1 min after the start of the equalization in the enclosure were used for getting the correlation. In this sense, this point was set to the initial point for getting the correlation. The pressure data were correlated by Eq. (1), as shown in Fig. 2(a). The parameters (a and b) were used to obtain the evaporation rate through the time-differentiation of Eq. (1):

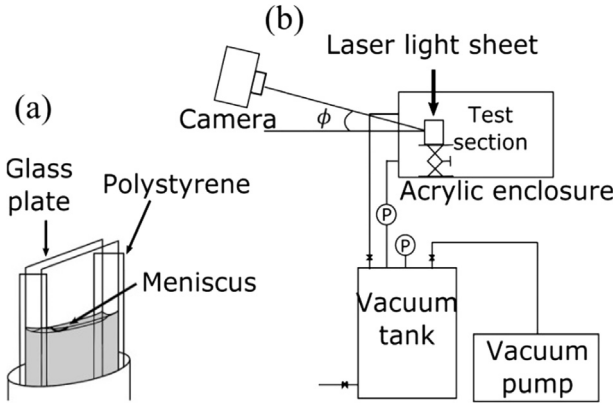

Fig. 1. (a) Test section. (b) Experimental apparatus.

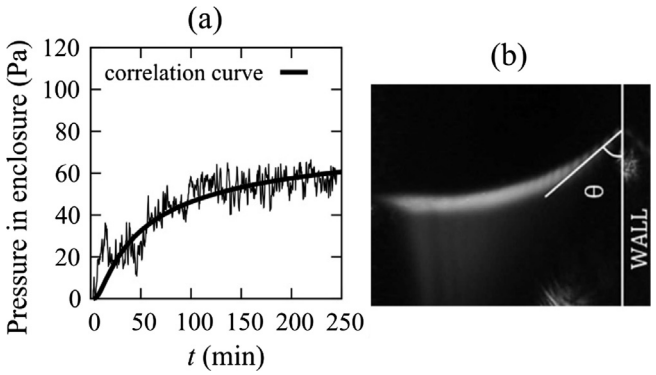

Fig. 2. (a) Time-evolution of differential pressure. (b) Image of meniscus.

$$dC/dt = MV(RT)^{-1}df/dt = abMV(RT\sqrt{\pi t^3})^{-1}\exp(-b^2/t). \quad (2)$$

Here, C, V, T, M and R are mass of the vapor phase (g), volume of vapor phase (m^3), temperature in the enclosure (K), molecular weight of water (g mol^{-1}) and gas constant (Pa m^3 mol^{-1} K^{-1}). As the simplicity of discussion, the vapor was assumed as an ideal gas. The evaporation flux could be obtained from the evaporation rate divided by the gap area.

In order to visualize the meniscus, a laser light sheet was used. The shape of meniscus at the equilibrium state was observed by a single-lens reflex camera (NIKON Corp.) coupled with the Cassegrain optical system (Seika Corp.). The spatial resolution of this system was adjusted as 0.9–1.4 μm $pixel^{-1}$. An example of the meniscus shape detection near the contact line was shown in Fig. 2(b). After detecting the contour of the meniscus through the image processing, the contact angle (θ in Fig. 2(b)) was analyzed by the FAMAS software (Kyowa Interface Science Co., Ltd.). The contact angle obtained was corrected by the angle between the axis of the camera and the horizontal plane (ϕ in Fig. 1(b)).

3. Experimental results

The parameters (a and b) for each gap distance are shown in Fig. 3(a) together with the standard error. Both a and b increased as the gap distance decreased. The parameter a is corresponding to the difference of the differential pressure between at $t = 0$ to ∞, in other words, total mass of the water evaporated in that time period. This result implies that the total mass of the evaporated water was increased with the decrease of the gap distance. The parameter b indicates how long it takes to reach the saturation pressure. If b is larger, it takes longer time to reach the saturation state, and vice versa. The result implies the increase of the resistance at the gap with the decrease of the gap distance.

As shown in Fig. 2(a), the differential pressure got close to the saturation about 1 h after the equalization. The evaporation rate and the evaporation flux at $t = 60$ min calculated by the pressure time-evolution data for each gap distance are shown in Fig. 3(b). The evaporation rate increased almost linearly with the decrease of the gap distance. The evaporation flux increased significantly with the decrease of the gap distance. The value at 0.30 mm-gap was about 40 times larger than that of 1.50 mm-gap case.

The evaporation rates and fluxes with the macroscopic curvature at $t = 6$ min are shown in Figs. 4 and 5 together with the experimental results obtained by using the capillary tubes [24]. According to [24], the evaporation fluxes of the volatile liquids (Ethanol, Methanol, Acetone, and Pentane) were referred to the spherical cap area, while it was defined by the gap area in this study. So, the evaporation fluxes of the volatile liquids were redefined by the tube area in Fig. 5 by assuming these liquids completely wet the wall. It is notable that the experiments [24] were

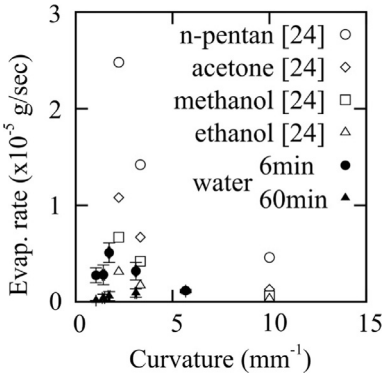

Fig. 4. Evaporation rate with curvature.

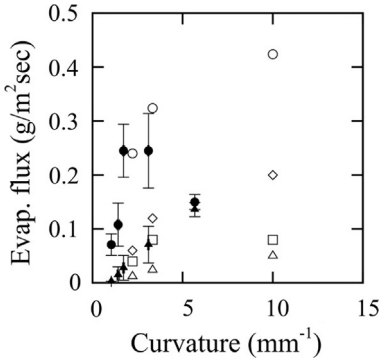

Fig. 5. Evaporation flux with curvature.

conducted in the open air, while the evaporation of water was caused by the pressure equalization in this study. At $t = 6$ min, the evaporation rates and fluxes of water are almost equivalent to those of the volatile liquids. The tendencies of the evaporation rate and flux at $t = 6$ min firstly increased nonlinearly as the curvature increased, while both of them reversely decreased above the curvature of 2 mm^{-1}. The increases of the evaporation rate and flux were resulted from the increase of the amount of evaporated liquid, on the other hand, the decrease was due to the increase of the resistance at the gap. When the evaporation process further proceeded, the resistance at the gap became small because the vapor pressure in the gap reached the saturation state, and then the evaporation rates and fluxes at $t = 60$ min increased as the curvature increased, as shown in Figs. 4 and 5. It was found that the tendencies of the evaporation rate are opposite between the existing data [24] and the present data at $t = 60$ min and at $t = 6$ min in the small curvature (less than 2 mm^{-1}). This inconsistency is supposed to come from which effect, of the curvature or of the

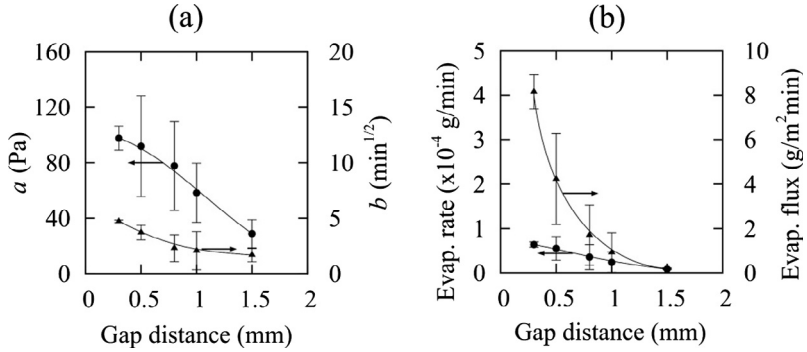

Fig. 3. (a) Variation of a and b with gap distance. (b) Evaporation rate and flux with gap distance.

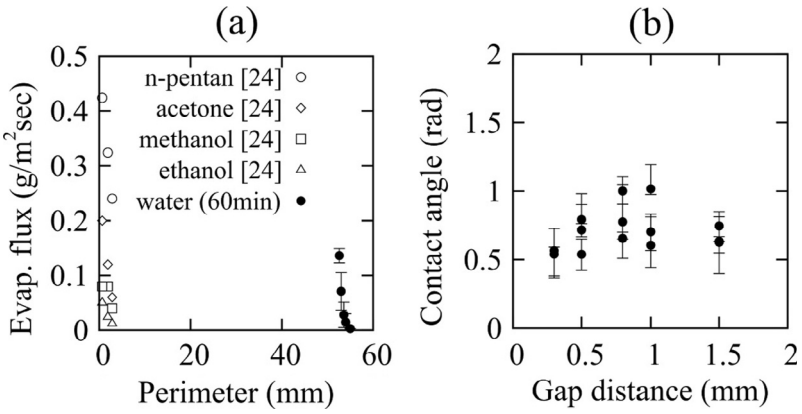

Fig. 6. (a) Evaporation flux with perimeter. (b) Apparent contact angle with gap distance.

contact-line length, is dominant in the evaporation process, as discussed in the next section.

Fig. 6(a) shows the variation of the evaporation fluxes at $t = 60$ min with the perimeter of the gap. The idea that the evaporation rate and flux could be determined by the contact-line length [29], led to the physically impossible result that the volatility of the water would be much greater than the "more volatile" liquids, even if considering the difference of the experimental condition. As shown in Figs. 4, 5 and 6(a), it is obvious that the evaporation rate and flux could be organized by the curvature, not the perimeter (i.e., not the contact-line length).

The available data of the apparent contact angle with various gap distances is shown in Fig. 6(b). The error of the contact angle depends on the smoothness of the contour of the meniscus, i.e. how clearly the meniscus image was taken. As shown in Fig. 6(b), the apparent contact angle in this study was around 0.6–0.9 rad.

4. Discussion

As shown in Fig. 3(a), the total mass of the evaporated water was increased with the increase of the macroscopic curvature. This result would be a clear evidence that the evaporation was enhanced by the curvature, and the increase of the total mass of the evaporated water led to the results that the evaporation rates and fluxes increased as the curvature increased at $t = 60$ min and $t = 6$ min (up to 2 mm^{-1}). As mentioned in Section 1, the existing data were strongly affected by the variation of the contact-line length (or perimeter), while the variation of the perimeter was so small in this study. This difference resulted in the opposite tendency found in Fig. 4. Generally, the characteristic length of the meniscus can be determined by either shorter one of the capillary length or the length of the system [30]. It is well-known that the capillary length in the water-air system is around 2 mm, so we conducted the experiments in small gap distance compared to the capillary length, which means that the surface curvature increases as the gap distance decreases. At the initial state of the meniscus, the liquid-vapor interface must be superheated to evaporate [12], and the degree of the superheat depends on the surface curvature. On the other hand, from a thermal penetration depth δ approximated by the equation below, the thermal relaxation time τ is about 0.2 s.

$$\delta = \sqrt{12\alpha\tau}. \quad (3)$$

Here, δ = 1.0 mm, which is the thickness of the glass plate, and α is a thermal diffusivity of the glass. This thermal relaxation time is much shorter than the time period of the pressure equalization, which was around 1 min. Considering that the test plate was not heated, the wall temperature is supposed to be the same as the liquid temperature in the initial condition (i.e., at the pressure equalization). Therefore, the evaporation was mainly caused by the surface curvature. As for the effect of the surface area, this is not the reason for the evaporation, because the area in the wide gap has small curvature, that is, low superheat at the surface. The curvature also affects the "apparent" resistance at the gap. Generally, if a mean free path of vapor molecule becomes long compared to the gap distance, the effect of the gap would appear as a diffusion resistance. However, Knudsen number in this experiment was about 10^{-3}, so the evaporated flow was assumed to be a continuum. This implies that the vapor did not receive the diffusion resistance at the gap in the high evaporation case. When the meniscus has small curvature or reaches the saturation state, the evaporation would follow the ordinary diffusion process.

5. Conclusions

The experiments were conducted to investigate the effect of the macroscopic curvature on the evaporation rate and the evaporation flux of water from the meniscus in the vertically parallel glass plates standing on the purified water pool. In the experiments, the curvature could be set to the desired value, while the variation of the perimeter was small. So the effect of the curvature was evaluated individually from the effect of the contact-line length. As the results, the total mass of the evaporated water increased as the curvature increased, so the evaporation rate and the evaporation flux could increase with the curvature. This result indicates the opposite trend against the experimental results obtained by other researchers, where the capillary tubes of the various diameters were used to evaluate the evaporation rate and flux from the meniscus. This inconsistency is because they could not evaluate individually the effect of the curvature from the effect of the contact-line length. Moreover, it was shown that the evaporation rate and flux could be organized with the curvature, not the perimeter (i.e., not the contact-line length). If the large temperature drop occurs at the meniscus due to the strong or rapid evaporation, the heat conduction effect of the wall may appear, and the heat/mass transport process would depend on it. So the heat conduction effect in the wall should be investigated further to reveal the whole physics in the phase change of the meniscus.

References

[1] M. Potash, P.C. Wayner, Evaporation from a two-dimensional extended meniscus, Int. J. Heat Mass Transfer 15 (1972) 1851–1863, http://dx.doi.org/10.1016/0017-9310(72)90058-0.

[2] K. Stephan, Influence of dispersion forces on phase equilibria between thin liquid films and their vapour, Int. J. Heat Mass Transfer 45 (2002) 4715–4725, http://dx.doi.org/10.1016/S0017-9310(01)00250-2.
[3] V.P. Carey, A.P. Wemhoff, Disjoining pressure effects in ultra-thin liquid films in micropassages—comparison of thermodynamic theory with predictions of molecular dynamics simulations, J. Heat Transfer 128 (2006) 1276–1284, http://dx.doi.org/10.1115/1.2349504.
[4] F. Renk, P.C. Wayner, G.M. Homsy, On the transition between a wetting film and a capillary meniscus, J. Colloid Interface Sci. 67 (1978) 408–414, http://dx.doi.org/10.1016/0021-9797(78)90229-1.
[5] P.C. Stephan, C.A. Busse, Analysis of the heat transfer coefficient of grooved heat pipe evaporator walls, Int. J. Heat Mass Transfer 35 (1992) 383–391, http://dx.doi.org/10.1016/0017-9310(92)90276-X.
[6] S. Moosman, G.M. Homsy, Evaporating menisci of wetting fluids, J. Colloid Interface Sci. 73 (1980) 212–223, http://dx.doi.org/10.1016/0021-9797(80)90138-1.
[7] A. Zou, A. Chanana, A. Agrawal, P.C. Wayner, S.C. Maroo, Steady state vapor bubble in pool boiling, Sci. Rep. 6 (2016) 20240, http://dx.doi.org/10.1038/srep20240.
[8] A.-M. Cazabat, G. Guéna, Evaporation of macroscopic sessile droplets, Soft Matter 6 (2010) 2591, http://dx.doi.org/10.1039/b924477h.
[9] K. Sieradzki, Curvature effects in alloy dissolution, J. Electrochem. Soc. 140 (1993) 2868–2872, http://dx.doi.org/10.1149/1.2220924.
[10] K.S. Glavatskiy, D. Bedeaux, Curvature dependence of the interfacial heat and mass transfer coefficients, J. Chem. Phys. 140 (2014) 1–12, http://dx.doi.org/10.1063/1.4867285.
[11] O. Wilhelmsen, D. Bedeaux, S. Kjelstrup, Heat and mass transfer through interfaces of nanosized bubbles/droplets: the influence of interface curvature, Phys. Chem. Chem. Phys. 16 (2014) 10573–10586, http://dx.doi.org/10.1039/C4CP00607K.
[12] S.J.S. Morris, The evaporating meniscus in a channel, J. Fluid Mech. 494 (2003) 297–317, http://dx.doi.org/10.1017/S0022112003006153.
[13] P.C. Wayner, Y.K. Kao, L.V. LaCroix, The interline heat-transfer coefficient of an evaporating wetting film, Int. J. Heat Mass Transfer 19 (1976) 487–492, http://dx.doi.org/10.1016/0017-9310(76)90161-7.
[14] S. DasGupta, J.A. Schonberg, I.Y. Kim, P.C. Wayner, Use of the augmented Young-Laplace equation to model equilibrium and evaporating extended menisci, J. Colloid Interface Sci. 157 (1993) 332–342, http://dx.doi.org/10.1006/jcis.1993.1194.
[15] H. Wang, Z. Pan, Z. Chen, Thin-liquid-film evaporation at contact line, Front. Energy Power Eng. China 3 (2009) 141–151, http://dx.doi.org/10.1007/s11708-009-0020-2.
[16] H. Wang, S.V. Garimella, J.Y. Murthy, Characteristics of an evaporating thin film in a microchannel, Int. J. Heat Mass Transfer 50 (2007) 3933–3942, http://dx.doi.org/10.1016/j.ijheatmasstransfer.2007.01.052.
[17] K. Park, K.S. Lee, Flow and heat transfer characteristics of the evaporating extended meniscus in a micro-capillary channel, Int. J. Heat Mass Transfer 46 (2003) 4587–4594, http://dx.doi.org/10.1016/S0017-9310(03)00306-5.
[18] K. Park, K.J. Noh, K.S. Lee, Transport phenomena in the thin-film region of a micro-channel, Int. J. Heat Mass Transfer 46 (2003) 2381–2388, http://dx.doi.org/10.1016/S0017-9310(02)00541-0.
[19] W. Qu, T. Ma, J. Miao, J. Wang, Effects of radius and heat transfer on the profile of evaporating thin liquid film and meniscus in capillary tubes, Int. J. Heat Mass Transfer 45 (2002) 1879–1887, http://dx.doi.org/10.1016/S0017-9310(01)00296-4.
[20] R.S.R. Gorla, L.W. Byrd, D.M. Pratt, Second law analysis for microscale flow and heat transfer, Appl. Therm. Eng. 27 (2007) 1414–1423, http://dx.doi.org/10.1016/j.applthermaleng.2006.10.027.
[21] C.A. Ward, F. Duan, Turbulent transition of thermocapillary flow induced by water evaporation, Phys. Rev. E 69 (2004) 56308, http://dx.doi.org/10.1103/PhysRevE.69.056308.
[22] G. Fang, C.A. Ward, Temperature measured close to the interface of an evaporating liquid, Phys. Rev. E 59 (1999) 417, http://dx.doi.org/10.1103/PhysRevE.59.417.
[23] S. Popov, A. Melling, F. Durst, C.A. Ward, Apparatus for investigation of evaporation at free liquid–vapour interfaces, Int. J. Heat Mass Transfer 48 (2005) 2299–2309, http://dx.doi.org/10.1016/j.ijheatmasstransfer.2004.10.038.
[24] C. Buffone, K. Sefiane, Investigation of thermocapillary convective patterns and their role in the enhancement of evaporation from pores, Int. J. Multiph. Flow 30 (2004) 1071–1091, http://dx.doi.org/10.1016/j.ijmultiphaseflow.2004.05.010.
[25] C. Buffone, K. Sefiane, IR measurements of interfacial temperature during phase change in a confined environment, Exp. Therm. Fluid Sci. 29 (2004) 65–74, http://dx.doi.org/10.1016/j.expthermflusci.2004.02.004.
[26] C. Buffone, K. Sefiane, Temperature measurement near the triple line during phase change using thermochromic liquid crystal thermography, Exp. Fluids 39 (2005) 99–110, http://dx.doi.org/10.1007/s00348-005-0986-4.
[27] C. Buffone, K. Sefiane, J.R.E. Christy, Experimental investigation of self-induced thermocapillary convection for an evaporating meniscus in capillary tubes using micro-particle image velocimetry, Phys. Fluids 17 (2005) 1–18, http://dx.doi.org/10.1063/1.1901688.
[28] C. Buffone, K. Sefiane, J.R.E. Christy, Experimental investigation of the hydrodynamics and stability of an evaporating wetting film placed in a temperature gradient, Appl. Therm. Eng. 24 (2004) 1157–1170, http://dx.doi.org/10.1016/j.applthermaleng.2003.10.038.
[29] K. Sefiane, C.A. Ward, Recent advances on thermocapillary flows and interfacial conditions during the evaporation of liquids, Adv. Coll. Interface. Sci. 134 (2007) 201–223, http://dx.doi.org/10.1016/j.cis.2007.04.020.
[30] P.G. de Gennes, F. Brochard-Wyart, D. Quéré, Gouttes, bulles, perles et ondes, Belin, 2002.